Am J Transl Res 2017;9(5):2219-2230
www.ajtr.org /ISSN:1943-8141/AJTR0043634

Original Article

Research on the traditional Chinese medicine treating gastrointestinal motility in diabetic rats by improving biomechanical remodeling and neuroendocrine regulation

Jiaxing Tian[1,2*], Min Li[2*], Jingbo Zhao[3*], Junling Li[4], Guifang Liu[2], Zhong Zhen[2], Yang Cao[1], Hans Gregersen[5,6], Xiaolin Tong[2]

[1]Graduate School, Beijing University of Chinese Medicine, Beijing 100029, China; [2]Department of Endocrinology, Guang'anmen Hospital, China Academy of Chinese Medical Sciences, Beijing 100053, China; [3]Department of Clinical Medicine, Aarhus University, Aarhus 8200 N, Denmark; [4]School of Traditional Chinese Medicine, Capital Medical University, Beijing 100069, China; [5]Bioengineering College of Chongqing University, Chongqing 400044, China; [6]GIOME, Department of Surgery, Chinese University of Hong Kong and Prince of Wales Hospital, Shatin, Hong Kong. [*]Co-first authors.

Received November 5, 2016; Accepted February 26, 2017; Epub May 15, 2017; Published May 30, 2017

Abstract: Previous studies have demonstrated that TWA, a Chinese herbal medicine, could significantly improve the symptoms of patients with diabetic gastrointestinal dysfunction. However, the specific mechanism of regulating intestinal peristalsis has not been found. This study aimed to discover TWA's therapeutic mechanism for regulating intestinal motility. The intestinal propulsion rate of diabetic rats was significantly increased after treatment with TWA for 8 weeks. Aiming at the mechanical structure, biomechanical testing indicated that TWA can significantly decrease the no-load intestinal wall thickness, cross-sectional area, and angular spread in a zero-stress state. Notably, intestinal stress-strain curve shifted to the right, which indicated TWA can inhibit intestinal hyperplasia and hardening and improve biomechanical remodeling. Further study of the mechanism revealed that TWA significantly inhibited the expression of AGE in the villi, crypt, and muscle and RAGE in crypt and upregulated the expression of nerve regulator (PSD95, C-kit and SCF). Radioimmunoassay showed TWA treatment decreased levels of serum somatostatin and vasoactive intestinal peptide. Moreover, associations were found between the intestinal propulsion rate with the morphologic and biomechanical remodeling parameters, changes of nerve factors, and endocrine hormones. Morphologic and biomechanical remodeling of the intestinal wall are the pathologic basis of gastrointestinal dysfunction. TWA can benefit intestinal motility by improving biomechanical and morphologic remodeling and by regulating expression of neuroendocrine factors. The results showed that the effect of TWA was dose-dependent, the higher the dose, the greater is the improvement. Thus, traditional Chinese medicine might be a valuable tool for treating diabetic gastrointestinal dysfunction.

Keywords: Diabetic gastrointestinal dysfunction, biomechanical remodeling, advanced glycation end products, neuroendocrine regulation, brain-gut peptide, TWA

Introduction

Gastrointestinal (GI) dysfunction is common in patients with diabetes during the disease's development, with symptoms arising from the whole GI tract. Common symptoms that patients report include postprandial fullness, nausea, vomiting, and bloating [1]. Previous studies have demonstrated that the GI dysfunction in patients with diabetes had a slow intestinal propulsion rate [2]. However, a lack of deep and systematic research exists on the mechanism of intestinal motility disorders in diabetes.

In recent years, studies have shown that the relationship between characteristics of intestinal biomechanical properties and physiologic functions was closely related. The remodeling of intestinal biomechanical properties occurred in diabetes mellitus (DM) [3]. Zhao and colleagues, through a series of studies, have found that DM induced histomorphological and biomechanical remodeling of the intestine with increasing intestinal wall stiffness in a time-dependent manner. The remodeling played an important role in DM GI dysfunction [4, 5].

It has been demonstrated that Tangweian decoction (TWA), a Chinese herbal medicine, could significantly improve the symptoms of nausea, vomiting, and abdominal distension, which markedly increased the quality of life in patients with diabetic GI dysfunction [6]. However, it was noted that TWA's effect on blood glucose was limited, which suggested that TWA may exert its efficacy through other mechanisms. Our previous study found that TWA could improve intestinal morphologic and biomechanical remodeling [7]. However, the specific mechanism of regulating intestinal peristalsis by TWA has not been studied.

Advanced glycation end products (AGEs) is the stable covalent compound formed by the non-enzymatic glycosylation combined with the aldehyde or carbonyl with the amino of protein [8], while high blood glucose would accelerate the aggregation of AGEs in the tissues. Its receptor (RAGE) is a transmembrane receptor of the immunoglobulin superfamily, which is compatible with AGE. Previous studies have demonstrated that the expression of AGE and RAGE increased in the small intestine and colon of DM rats [3, 9]. Therefore, the non-enzymatic glycosylation in GI tissue induced by sustaining high glucose may be one of the important mechanisms for intestinal remodeling and the intestinal peristalsis disorders.

The enteric nervous system (ENS) is involved in the pathogenesis of GI dysfunction, and the impairment of synaptic transmission function plays a key role in the disease [10, 11]. Postsynaptic density protein 95 (PSD95), one of the most expressed proteinsin postsynaptic density, influences the synaptic structure and remodeling function [12, 13]. Previous studies have confirmed that the expression of PSD95 decreased during DM development [14]. High glucose leads to impairment of ENS transmission function, which could affect the intestinal peristalsis.

Interstitial cells of Cajal (ICCs) generate pacemaker signals in the GI tract. The tyrosine kinase receptor (C-Kit) is one of the membrane receptors of ICCs, and its ligand is stem cell factor (SCF). The study has confirmed that the C-Kit-SCF signaling pathway was impaired in DM, which could affect the proliferation and differentiation of ICCs that leads to intestinal dysfunction [15, 16]. Gaddipati et al has proposed that brain gut peptides (BGPs), a class of peptides distributed both in the GI tract and brain, were also involved in the regulation of GI motility [17, 18]. The hormones secreted by endocrine cells released into the blood to act on the target organ and play a regulation role. The hormones can also affect the adjacent cells by paracrine. In addition, many BGPs are also neurotransmitters, which play a role through releasing by the nerve endings [19]. Somatostatin (SS) and vasoactive intestinal peptide (VIP) are two important BGPs, and changes in their levels may lead to GI dysmotility [20]. Therefore, the secretion disorder of the neuroendocrine factors in DM is also one of the mechanisms of intestinal peristalsis disorders.

Thus, we speculated that TWA could promote intestinal motility of diabetic rats by improving biomechanical remodeling and regulating neuroendocrine factors. This study's purpose is to explore the mechanism of regulating intestinal peristalsis by TWA based on biomechanical remodeling and neuroendocrine regulation.

Materials and methods

Materials

TWA is composed of fructus aurantii immaturus, rhizoma atractylodis macrocephalae, rhubarb, pinellia ternate, ginger, peach kernel, and codonopsispilosula. It was generated at the Department of Pharmacy of Guang'anmen Hospital (Beijing, China). There were quantitative control limits for the raw herbs. TWA's chemical composition has been determined by ultra-fast high performance liquid chromatography-electrospray-ionization-quadrupole time-of-flight mass spectrometry method [7]. Streptozocin was purchased from Sigma-Aldrich Co. LLC (St Louis, MO, USA). Chloral hydrate and sodium citrate were purchased from Sinopharm Chemical Reagent Co., Ltd (Beijing, China). Glycosylated serum protein (GSP) fructosamine kit was purchased from Nanjing Mindit Biochemistry Co., Ltd (Nanjing, China). Ink was purchased from Shanghai Fine Stationery Co., Ltd. (Shanghai, China). SS radioimmunoassay (RIA) kit and VIP RIA kit were purchased from Beijing Sino-UK Institute of Biological Technology Co., Ltd. (Beijing, China).

Animals and experimental design

All experiments were approved by the Local Ethics Committee for Animal Research Studies

at the Guang'anmen Hospital. Adult male Wistar rats (Beijing HFK bioscience CO., LTD, QC NO. SCXK 2009-007), weighing 180 to 220 g, were kept in specific pathogen-free laboratory and with free access to water throughout the experiments. They were housed in a restricted access room with controlled temperature (22° to 25°C) and a light/dark (12 h:12 h) cycle. DM was induced in 64 rats by a single intraperitoneal injection of 60 mg/kg body weight of streptozocin (STZ, Sigma-Aldrich). This dose of STZ resulted in a random blood glucose level ≥16.7 mmoL/L in 72 h after the injection. STZ-induced diabetic rats were subdivided into 4 groups (16 in each group)-i.e., DM group, TWA high dose group (H), TWA medium dose group (M), and TWA low dose group (L). Another 16 rats of similar age and body weight from the same vendor were used as a normal control group (NC). TWA was administered once daily from the beginning of the experiment by gavage, which passed though the esophagus and directly reached the stomach lumen. The dosage was 15 g/kg for H, 10 g/kg for M, and 5 g/kg for L. The rats in the DM and NC groups were perfused with physiologic saline.

The experimental period was 8 weeks. At the end of the experiment, the rats were fasted overnight and anesthetized with 10% chloral hydrate (3.5 mL/kg, ip). Half the rats (40 rats, 8 rats for each group) were used to determine intestinal propulsion rate. Another half of the rats (40 rats, 8 rats for each group) were used to analyze: 1) morphometric and biomechanical tests, 2) the expressions of advanced glycation end-products (AGEs) and its receptors, and 3) the expressions of neuroendocrine factors. For the second set of experiments, about a 10-cm long jejunal segment from 5 cm distal to the ligament of Treitz was taken out. From proximal to distal, the tissue was used for immunohistochemistry, RT-PCR analysis, western blot analysis, zero-stress state determining, and distension testing.

Glycometabolism examinations

The rats were weighed weekly and monitored for glucose from tail vein at 4 weeks and 8 weeks after initiating the experiment. For blood glucose measurement, one drop of blood was obtained from the tail vein, and blood glucose was measured by a Johnson & Johnson One Touch Ultra Blood Glucose Meter. For GSP measurement, blood was obtained from the abdominal aorta, and serum was separated. GSP was measured by fructosamine (GSP fructosamine kit, Nanjing Mindit Biochemistry Co., Ltd., China) at the end of the experiment.

Intestinal propulsion rate testing

The rats fasted overnight and received an oral administration of 1 ml/100 g carbonic ink. After 30 min, the rats were anesthetized with 10% chloral hydrate (3.5 mL/kg, ip) and the complete intestinal tract, from the pylorus to the terminal rectum, was removed. The lengths of the whole intestinal tract and the distance of ink propulsion were measured. The percentage of blackened intestinal tracts was calculated: intestinal propulsion rate (%) = pushing length/total length × 100%.

Biomechanical testing

To determine zero-stress state: To obtain data on the zero-stress state, three 1 to 2 mm wide intestinal rings were cut and placed in Krebs solution at room temperature. The composition of Krebs solution (mmol/L) was: NaCl, 118; KCl, 4.7; $NaHCO_3$, 25; NaH_2PO_4, 1.0; $MgCl_2$, 1.2; and ascorbic acid, 0.11. A photograph was taken of the cross-section of the rings using a Canon camera (Canon, Japan) and was presented as the no-load state. Each ring-shaped segment was then cut radially from the opposite mesentery site, and photographs were taken about 60 min after the radial cutting to allow viscoelastic creep to take place. This is presented as the zero-stress state.

Distension test: A 5-cm long jejunal segment was cut and put in the Krebs solution. The papaverine was used to inhibit smooth muscle contraction for 30 min. Then, the jejunal segment was tied and inflated with Krebs solution using a distension protocol from 0 to 9 cm H_2O three times. The change in outer diameter of the jejunal segment was recorded by camera (Canon, Japan), while the change in pressure was measured by pressure sensor.

Mechanical data analysis

Morphometric data were obtained from digitized images in the jejunal tissue rings of zero-stress and no-load states. Measurements were undertaken using image analysis software (Sigmascan ver. 4.0, Sigma Corp., San Rafael, CA, USA). The following data were measured

from each specimen: circumferential length (C), wall thickness (h), wall area (A), and the opening angle at zero-stress state (α). The subscripts i, o, n, and z refer to the inner (mucosal) surface, outer (serosal) surface, no-load state, and zero-stress state. The measured data were used to calculate biomechanical parameters defined as:

Residual Green's strain at the mucosal surface:

$$E_i = \frac{(\frac{C_{i-n}}{C_{i-z}})^2 - 1}{2} \quad (1)$$

Residual Green's strain at the serosal surface:

$$E_o = \frac{(\frac{C_{o-n}}{C_{o-z}})^2 - 1}{2} \quad (2)$$

Stress-strain data analysis: Calculations were performed by the known data of no-load state, zero-stress state and pressurized condition. The Kirchhoff 's stress and Green's strain in a wall at a given pressure were calculated according to the following equations: The meaning of ΔP, r_{o-p}, r_{i-p}, h_p, and λ_θ refer to pressure, inner radius, outer radius, wall thickness, and the circumferential stretch ratio.

Circumferential mid-wall Green's strain:

$$E_\theta = \frac{\lambda_\theta^2 - 1}{2} \quad (3)$$

Circumferential Kirchhoff 's stress:

$$S_\theta = \frac{\triangle Pr_{i-p}}{h_p \lambda_\theta^2} \quad (4)$$

Immunohistochemical staining

Each rat's intestinal tissue was harvested and immediately fixed in 10% buffered formalin overnight. Samples were embedded in paraffin. The sections were flattened, mounted, and heated on the glass slides. After deparaffinization and dehydration, the sections were treated with H_2O_2 (3% in ethanol, room temperature, 15 min), and the sections were incubated with 5% BSA-PBS buffer (room temperature, 30 min) for blocking nonspecific staining. Afterwards, the sections were incubated with the primary anti-AGE antibody (Abcam, 1:300, diluted in 1% BSA-PBS) over night at 4°C. The sections were washed by PBS (0.01 mol/L) three times and for 3 min each. The sections were then incubated with PV-6000 (ZSGB-BIO) at room temperature for 15 min. The sections were then washed again as before and were immersed with DAB for 2 min. The primary anti-RAGE antibody was diluted (1:200) with 1% BSA-PBS. Other processes were similar to the AGE immunostaining. To evaluate the expression of AGE and RAGE, two independent pathologists who were blinded to the animal data examined and scored all slides. Images of the different parts, including villus, crypt, mucosa, and muscle layer, were taken separately. The region of interest was defined using NIS-Element image analysis software (Nikon, Japan). The color due to immunohistochemical staining was distinguished in the region of interestusing intensity thresholds. Finally, the images were exported as binary images and the area fraction of AGE or RAGE positive staining was determined. The fraction of AGE and RAGE were computed as follows: Fraction of AGE or RAGE = immuno-positive area/total measuring area.

RNA preparation and RT-PCR analysis

The jejunal tissue was frozen at -80°C. Total RNA was isolated from rat intestinal tissues with trizol reagent (Invitrogen, Carlsbad, CA, USA) and reverse-transcribed into cDNA using a Reverse Transcription System (Fermentas, part of Thermo Fisher Scientific, Waltham, MA, USA). The thermal cycling conditions were as follows: 95°C for 10 min followed by 35 cycles at 95°C for 25 s, 55°C for 25 s, 72°C for 50 s, and 72°C for 8 min. The mRNA expressions levels of C-kit, SCF, and PSD95 were quantitatively analyzed and normalized to GAPDH levels. The forward and reverse primer sequences wereas follow. SCF Forward: 5'-CCTCGTGGCATGTATGGAAG-3', Reverse: 5'-GCTGCAACAGGGGGTAACAT-3'; C-KIT Forward: 5'-CAAGAAGAACAGGCAGACGC-3', Reverse: 5'-TCCCAGAGGAAAATCCCATA-3'; PSD95 Forward: 5'-AAGACCGTGCCAACGATGA-3', Reverse: 5'-TGAGGGACACAGGATCCAAAC-3'; GAPDH Forward: 5'-TGCCTTCTCTTGTGACAAAGTGG-3', Reverse: 5'-CATTGCTGACAATCTTGAGGGAG-3'.

Western blot analysis

The jejunal tissue was frozen at -80°C. Protein extracts from rat intestinal tissues were quantified using the bicinchoninic acid method, separated by using 10% sodium dodecyl sulphate-polyacrylamide gel electrophoresis, and then transferred to polyvinylidene difluoride membranes (MilliporeCorp., Billerica, MA, USA). Non-

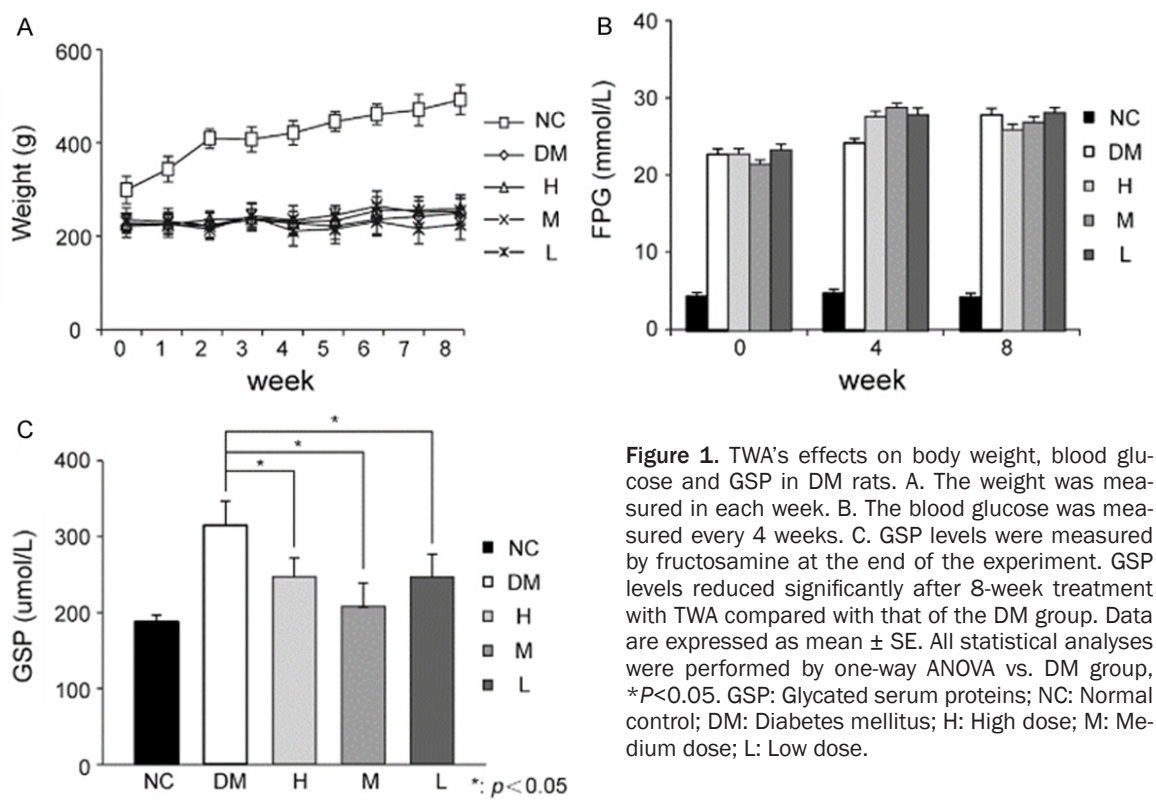

Figure 1. TWA's effects on body weight, blood glucose and GSP in DM rats. A. The weight was measured in each week. B. The blood glucose was measured every 4 weeks. C. GSP levels were measured by fructosamine at the end of the experiment. GSP levels reduced significantly after 8-week treatment with TWA compared with that of the DM group. Data are expressed as mean ± SE. All statistical analyses were performed by one-way ANOVA vs. DM group, **P*<0.05. GSP: Glycated serum proteins; NC: Normal control; DM: Diabetes mellitus; H: High dose; M: Medium dose; L: Low dose.

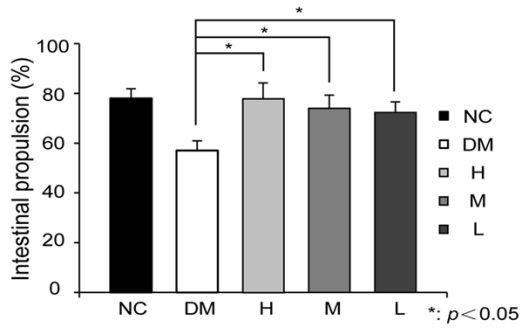

Figure 2. TWA's effects on intestinal propulsion rate in DM rats. Intestinal propulsion rate increased significantly in the different TWA groups after 8-week treatment. Data are expressed as mean ± SE. One-way ANOVA was performed to evaluate the difference vs. DM group, **P*<0.05. NC: Normal control; DM: Diabetes mellitus; H: High dose; M: Medium dose; L: Low dose.

specific binding was blocked with 5% no-fat milk in TBST buffer for 2 h at room temperature. The membranes were incubated with primary antibody against C-kit (1:500), SCF (1:1000), and PSD95 (1:1000) overnight at 4°C and then incubated with the horseradish peroxidase-conjugated secondary antibodies. Finally, the blots were visualized using an enhanced chemiluminescence detection kit (Millipore), and GAPDH was used as a loading control. Each experiment was repeated three times independently.

Serum BGP detection

For BGP measurement, blood was obtained from the abdominal aorta, and serum was separated. The serum SS and VIP were measured by radioimmunoassay (Beijing Sino-UK Institute of Biological Technology Co., Ltd, China) at the end of the experiment.

Statistical analysis

All the data are presented as mean ± SD and analyzed by one-way analysis of variance using SPSS19 software (SPSS Inc., Chicago, IL, USA). The constants a and b obtained from the exponential function ($S=(S^*+b)e^{a(E-E^*)}-b$) were used for the statistical evaluation of the stress-strain data. Where S is the stress, E is the strain, and S^* and E^* are the stress and the strain at an arbitrary point on the stress-strain curve. The linear regression analysis was used to analyze

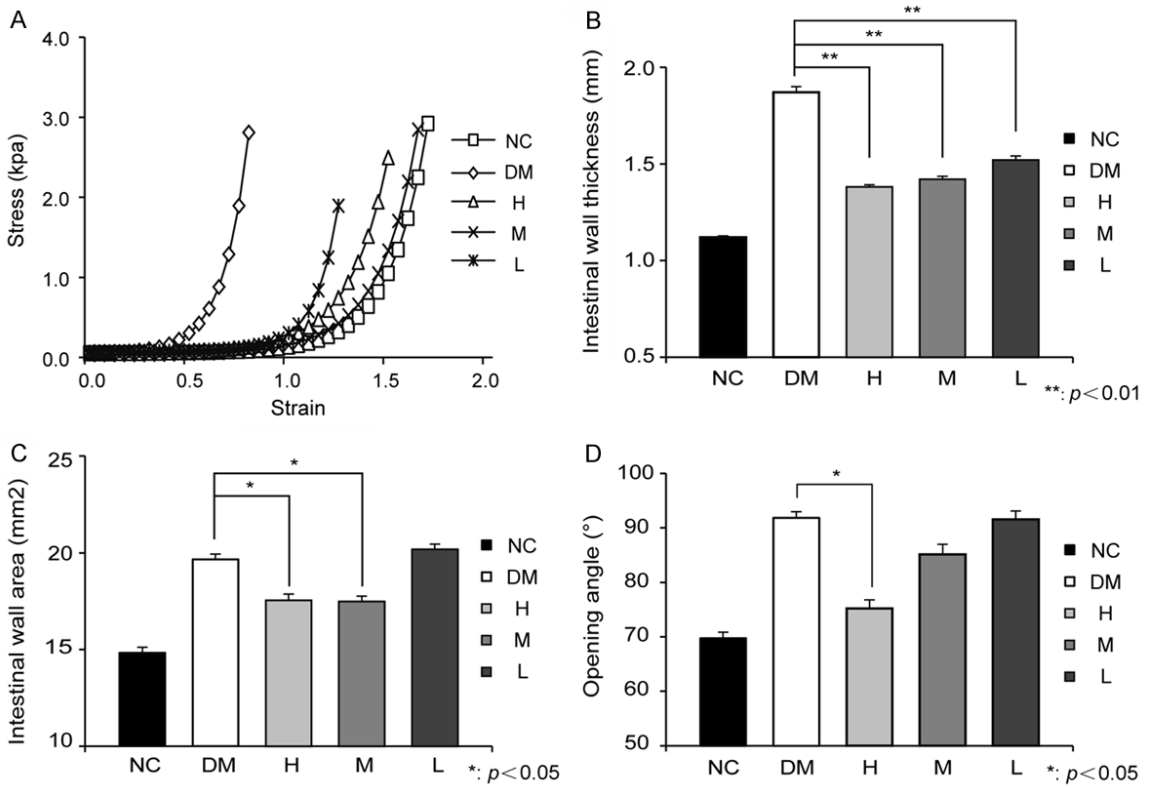

Figure 3. TWA's effects on morphometric biomechanical remodeling in DM rats. A. Intestinal stress-strain curves of TWA treatment groups shifted to the right compared with DM group, indicating decreased wall stiffness. B. Wall thickness significantly decreased in all three groups receiving TWA treatment. C. The wall area decreased significantly in the high- and middle-dose groups. D. The opening angle was increased in the DM group compared with the control group, and treatment with high-dose TWA decreased the opening angle significantly. Data are expressed as mean ± SE. All statistical analyses were performed by one-way ANOVA vs. DM group, **P*<0.05; ***P*<0.01. NC: Normal control; DM: Diabetes mellitus; H: High dose; M: Medium dose; L: Low dose.

the associations between intestinal propulsion rate and other parameters. P<0.05 was considered statistically significant.

Results

Changes in weight and glycometabolism

Compared with the body weight of the NC group, the body weight of DM rats decreased rapidly, and the weight had not significantly increased after treatment with TWA, indicating TWA did not significantly affect the body weight (**Figure 1A**). The fasting plasma glucose and GSP were significantly higher in the DM group than in the NC group (P<0.05; **Figure 1B**, **1C**). Compared with the DM group, there was no significant changes in fasting plasma glucosein the treatment groups (P>0.05; **Figure 1B**); however, the GSP had a significantly decreased after 8-week treatment with TWA (P<0.05; **Figure 1C**).

Changes in intestinal propulsion rate

Compared with the NC group, the intestinal propulsion rate of DM rats had a significant decrease (P<0.05, **Figure 2**). After 8-week treatment with TWA, the intestinal propulsion rate increased significantly in the different TWA groups (P<0.05), indicated that the drug could improve intestinal motility.

Changes in biomechanical and morphometry parameters

At the end of the experiment, the stress-strain analysis showed that the stress-strain curve of jejunal segments in the DM group shifted to the left compared with that in the control group, indicated that the diabetic intestinal wall became stiffer. Intestinal stress-strain curves of the TWA treatment group shifted to the right, which suggested that TWA could improve the biomechanical remodeling and decrease

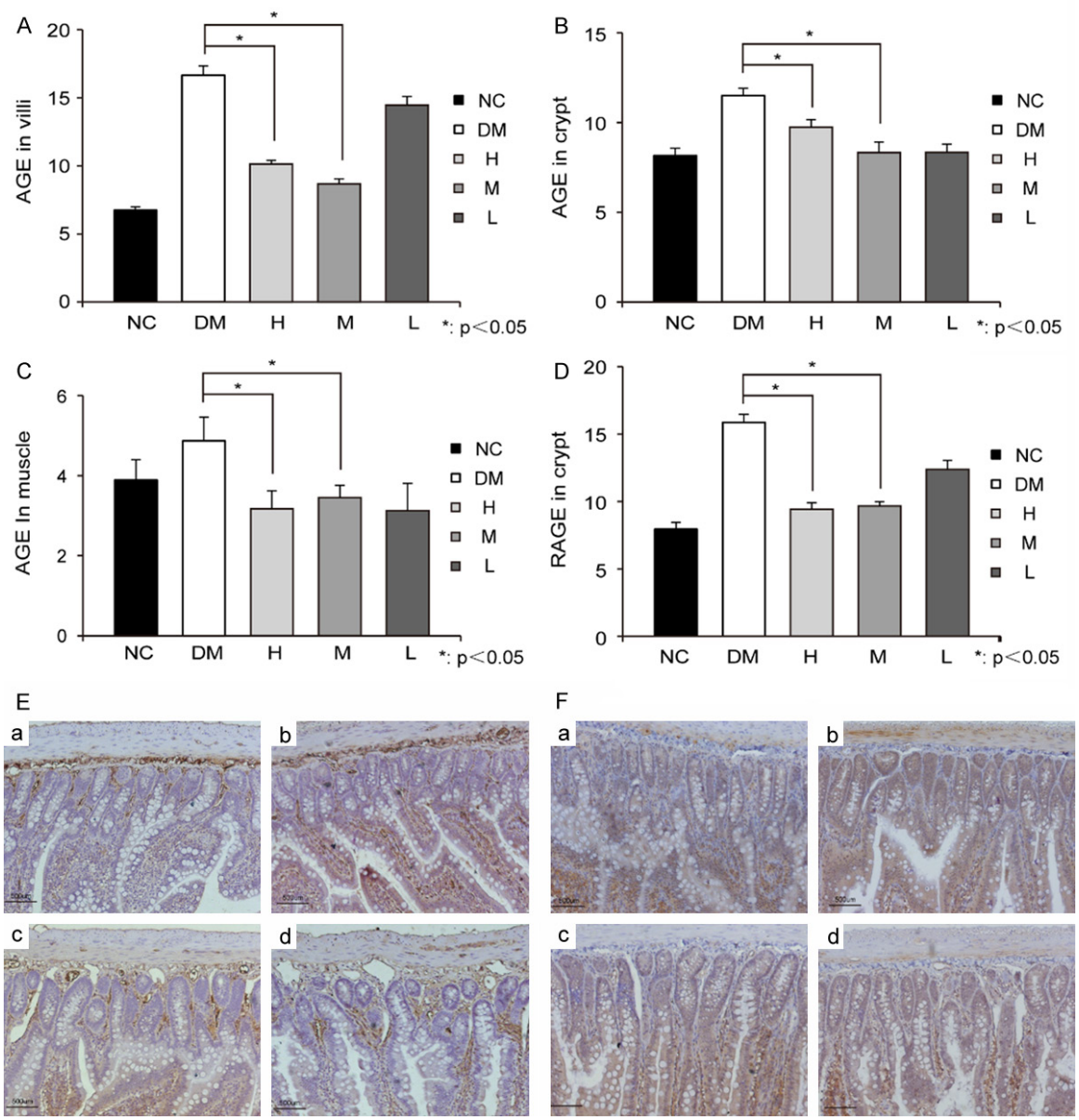

Figure 4. TWA's effects on immunohistochemical staining in DM rats. The immuno-positive area of AGE and RAGE were yellow-brown. The expression of AGE in the intestinal (A) villi, (B) crypt epithelial cells, and (C) muscle layer decreased after 8-week treatment with TWA in high- and middle-dose groups. (D) The reductions of RAGE in crypt epithelial cells were statistically significant in high- and middle-dose groups. All statistical analyses were performed by one-way ANOVA. (E) Examples of AGE immunostaining (a: NC, b: DM, c: H, d: L). (F) Examples of RAGE immunostaining (a: NC, b: DM, c: H, d: L) vs. DM group, *P<0.05. NC: Normal control; DM: Diabetes mellitus; H: High dose; M: Medium dose; L: Low dose.

the wall stiffness (P<0.05, **Figure 3A**). The M and H groups had better effect than the L group. Intestinal no-load wall thickness and cross-sectional wall area increased in the DM group compared with the control group (P< 0.01). After treatment with TWA, wall thickness was significantly decreased in all three groups that underwent TWA treatment (P< 0.01, **Figure 3B**), and the wall area decreased significantly in high and middle dose groups (P<0.05, **Figure 3C**), which showed that TWA could inhibit the intestinal wall proliferation and improve morphologic remodeling. At the end of the experiment, the opening angle was increased in the DM group compared with that in the control group (P<0.05). Treatment with high-dose TWA decreased the opening angle significantly (P<0.05; **Figure 3D**).

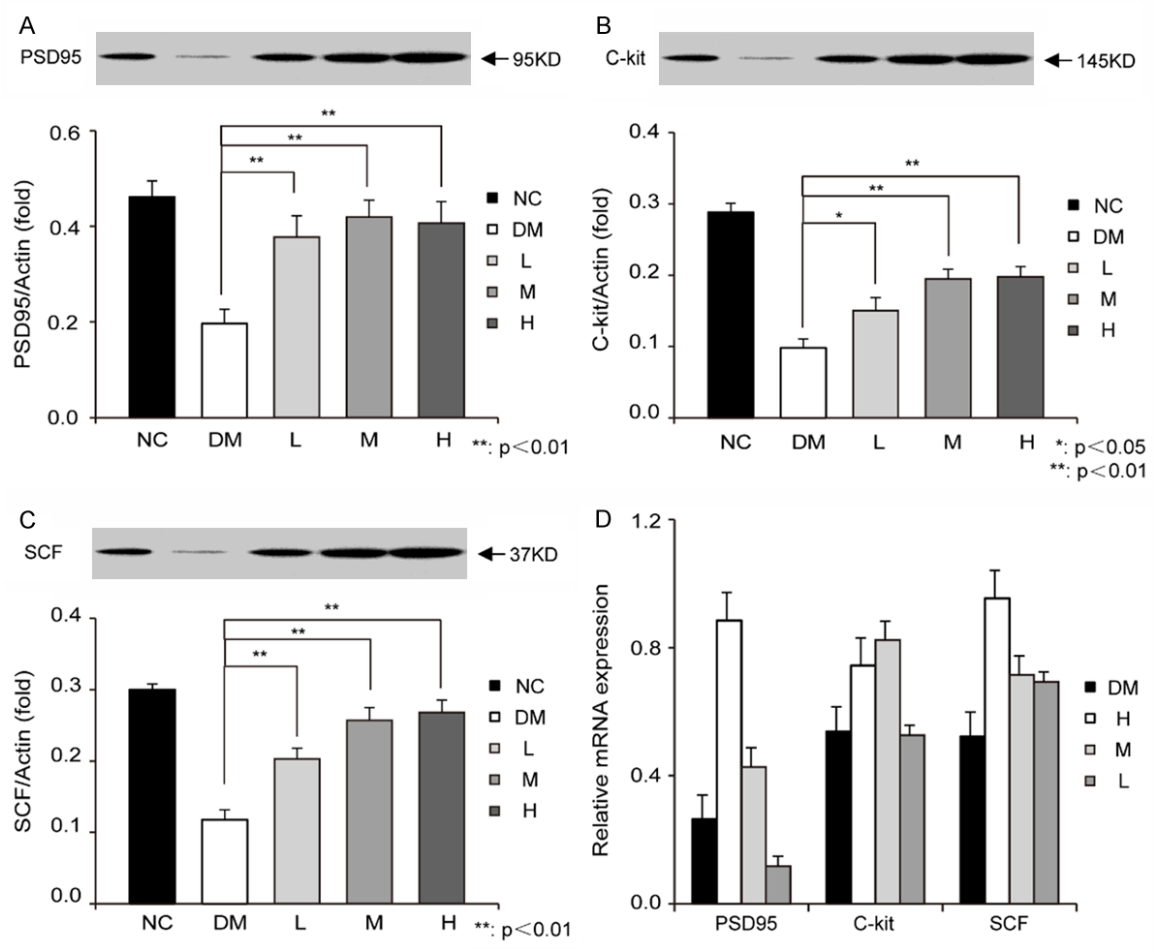

Figure 5. TWA's effects on basic functional unit of intestinal motility in DM rats. The proteinlevels of (A) PSD95, (B) C-kit, and (C) SCF were detected by western blotting. TWA treatment increased the protein levels of PSD95, C-kit and SCF in a dose-dependent manner, showing that TWA could significantly improve the basic functional unit of small-intestinal motility of DM rats. (D) The expression of PSD95, C-kit, and SCF mRNA showed a similar trend in relation to protein levels. All statistical analyses were performed by one-way ANOVA vs. DM group, **P*<0.05; ***P*<0.01. NC: Normal control; DM: Diabetes mellitus; H: High dose; M: Medium dose; L: Low dose.

Changes in distributions of AGE and RAGE

The immuno-positive area of AGE was yellow-brown (**Figure 4E**). These colors were not found in the negative control slides (data were not shown), demonstrating that the stained color was AGE specific. The expression of AGE was detected in the intestinal villi and crypt epithelial cells, submucosa, and muscle layer. The basal surface of villi epithelial cells and the basal part of crypt epithelial cells was stained stronger. After treatment with TWA, the expression of AGE in the intestinal villi, crypt epithelial cells, and muscle layer decreased in the high- and middle-dose groups (P<0.05, **Figure 4A-C**).

The immuno-positive area of RAGE was yellow-brown (**Figure 4F**). The expressions of RAGE were found in the intestinal villi, crypt epithelial cells, muscle layer, and nerve cells of ganglion. The intestinal villi cells stained stronger than the crypt epithelial cells. After treatment with TWA, the expressions of RAGE in the intestinal villi, crypt epithelial cells, and submucosa decreased in treatment groups. The reductions incrypt epithelial cells were statistically significant in the high- and middle-dose groups (P<0.05, **Figure 4D**).

Changes in the basic functional unit of intestinal motility

The protein levels of PSD95, C-kit, and SCF decreased in the DM group compared to the control group (P<0.01; **Figure 5A-C**). TWA treatment increased the protein levels of PSD95 in a dose-dependent fashion (P<0.01, **Figure 5A**), C-kit (P<0.05 and P<0.01, **Figure 5B**), and SCF

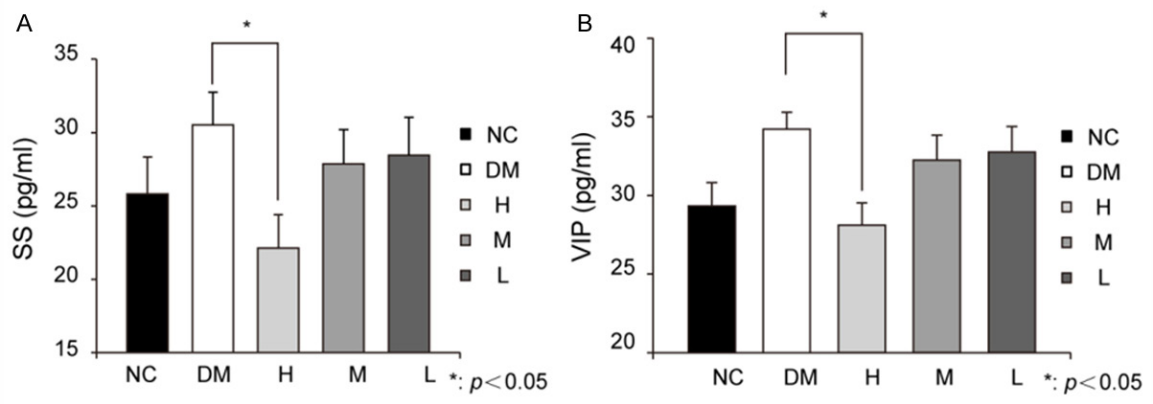

Figure 6. TWA's effects on serum SS and VIP in DM rats. The levels of serum (A) SS and (B) VIP were significantly increased in the DM group. SS and VIP declined in a dose-dependent manner in the treatment groups. SS and VIP were significantly reduced in thehigh-dose group compared with the DM group. Data are expressed as mean ± SE. All statistical analyses were performed by one-way ANOVA vs. DM group, *P<0.05. SS: Somatostatin; VIP: Vasoative intestinal peptide; NC: Normal control; DM: Diabetes mellitus; H: High dose; M: Medium dose; L: Low dose.

(P<0.01, **Figure 5C**), which showed that TWA could significantly improve the basic functional unit of small-intestinal motility of DM rats. The PCR results showed a similar trend in regulating those molecules in different groups (**Figure 5D**).

Changes in brain gut peptides expressions

Serum SS and VIP were significantly increased (P<0.05, **Figure 6**) in the DM group. Among the treatment groups, SS and VIP dosage-dependence declined. SS and VIP significantly reduced in the high-dose group compared with that in the DM group (P<0.05, **Figure 6**).

Associations between intestinal propulsion rate and other parameters

The linear regression analysis showed that changes in the intestinal propulsion rate were negatively associated with AGE expressions in villi epithelial cells and muscle layer, RAGE expressions in crypt epithelial cells, glucose level, intestinal wall thickness and area, opening angle, constant, and levels of BGPs, whereas the body weight, protein levels of PSD95, C-kit, and SCF were positively associated with the intestinal propulsion rate. R value ranged from 0.371 to 0.545, and F value ranged from 4.312 to 12.334 (P<0.05).

Discussion

In a previous study, we demonstrated that the symptom improvement after TWA treatment in patients with diabetic GI dysfunction was not by glucose control [6], and intestinal morphologic and biomechanical remodeling effect of TWA was observed [7]. In this study, we further confirmed that the intestinal morphologic and biomechanical remodeling occurred in DM rats [21, 22]. After TWA intervention, intestinal propulsion rate in DM rats increased in a dose-dependent manner, and the intestinal morphologic and biomechanical remodeling were significantly improved. It is necessary to reveal the mechanism behind these occurrences.

TWA partly improved morphology, including the increase in intestinal wall thickness and cross-sectional area, while biomechanical remodeling included a decrease in the opening angle and the shift of stress-strain curve to the right, indicating the intestinal elasticity increased and the stiffness decreased. The blood glucose levels were not obviously changed, as we reported previously. The morphologic changes in DM could alter the relative position of intestinal mechanosensitive nerve endings, while the biomechanical remodeling could change the stress distribution around the mechanosensitive nerve endings. These two factors influence the function of GI motility and sensory [23]. The morphology and biomechanical remodeling in DM were partially reversed by TWA intervention; therefore, the intestinal propulsion rate was promoted.

The accumulation of AGE in tissues would alter the structure and function of the matrix protein

[24]. Our previous study confirmed that the expression of AGE and its receptors in the small intestine and colon were up-regulated in DM rats [25], which suggested that non-enzymatic glycation in GI tissues may be one of the important mechanisms for GI remodeling [26]. After TWA intervention, the expression of AGE and RAGE in different intestinal layers decreased, especially in the villi epithelial cells for AGE and in the crypt epithelial cells for RAGE. The intestinal remodeling is closely related to the overexpression of AGE and its receptors. The up-regulation of AGE and RAGE in the DM intestinal mucosa may also affect the function of mucosal cell membrane and digestive enzyme activity [27-29].

Apart from the biomechanical structure, intestinal peristalsis is also regulated by neuroendocrine. PSD95 is a cytoskeletal network protein of nerve cell membrane. It is located in the pathway of synaptic ion flow, which regulates the interaction between the postsynaptic signaling molecule and the target molecule [30, 31]. The morphology and structure of PSD95 have great plasticity and mutability, which is important for postsynaptic structural development and reckoned as a morphologic parameter [32-34]. Previous studies reported that PSD95 plays an important role in the recovery of neurologic diseases by remodeling synaptic structure [35-38]. This study showed that TWA could alleviate the decreasing PSD95 expressions in the small-intestine tissue of DM rats, which indicated that the drug promotes GI peristalsis by improving synaptic changes of ENS.

ICCs operate as pacemakers in the GI tract. C-Kit is one of the membrane receptors of ICCs, and SCF is its ligand. The signaling pathway of SCF-C-Kit is closely related to ICCs [15, 16]. This study confirmed that impaired SCF-C-Kit signaling pathway in DM could affect the proliferation and differentiation of ICCs, which leads to decreased intestinal propulsion rate, destruction of intestinal contraction rhythm, and motility dysfunction [39-42]. TWA intervention can recover the motility and restore the rhythm of intestinal contraction by increasing the protein levels of C-kit and SCF.

SS is a BGP with suppression of pancreatic exocrine secretion and bile secretion. It also inhibits intestinal motility, which could cause constipation [20, 43, 44]. VIP is a kind of secretin family of GI peptide, which suppresses GI motility by inhibiting intestinal contraction and spontaneous pylorus contraction [45-49]. Our study found that TWA can decrease serum SS level and VIP, regulate the intestinal motility and GI dysfunction, along with other neuroendocrine factors.

In conclusion, in this study we confirmed that the morphometric and biomechanical remodeling and the upregulationof AGE and RAGE were observed in diabetic intestine. The neuroendocrine factors in the small intestine and the serum were also changed in diabetic rats. Those changes were associated with decreasing intestinal propulsion rate. TWA treatment can recover intestinal morphometric and biomechanical remodeling in DM rats and rebalance the expression and secretion of neuroendocrine factors. TWA plays a role in promoting intestinal peristalsis of DM rats. Our study provides new thinking that the Chinese herbal medicine maybe a good choice to treat diabetic GI dysfunction.

Acknowledgements

The study was supported by the National Natural Science Foundation of China (No. 8117-3259).

Disclosure of conflict of interest

None.

Address correspondence to: Xiaolin Tong, Department of Endocrinology, Guang'anmen Hospital, China Academy of Chinese Medical Sciences, Beijing 100053, China. E-mail: xiaolintong66@sina.com

References

[1] Kashyap P, Farrugia G. Diabetic gastroparesis: what we have learned and had to unlearn in the past 5 years. Gut 2010; 59: 1716-1726.

[2] Wang CL, Zhou Y, Guo C, Zhang Y, Wang R. In vivo characterization of intestinal effects of endomorphin-1 and endomorphin-2 in type 1 diabetic mice. Eur J Pharmacol 2013; 698: 499-504.

[3] Chen P, Zhao J, Gregersen H. Up-regulated expression of advanced glycation end-products and their receptor in the small intestine and colon of diabetic rats. Dig Dis Sci 2012; 57: 48-57.

[4] Zhao J, Chen P, Gregersen H. Stress-strain analysis of contractility in the ileum in response to flow and ramp distension in streptozotocin-induced diabetic rats--association with advanced glycation end product formation. J Biomech 2015; 48: 1075-1083.
[5] Zhao J, Chen P, Gregersen H. Stress-strain analysis of jejunal contractility in response to flow and ramp distension in type 2 diabetic GK rats: effect of carbachol stimulation. J Biomech 2013; 46: 2469-2476.
[6] Li JL, Li M, Pang B, Zhou Q, Tian JX, Liu HX, Zhao XY, Tong XL. Combination of symptoms, syndrome and disease: treatment of refractory diabetic gastroparesis. World J Gastroenterol 2014; 20: 8674-8680.
[7] Liu GF, Zhao JB, Zhen Z, Sha H, Chen PM, Li M, Zhang JC, Yuan MZ, Gao W, Gregersen H, Tong XL. Effect of tangweianjianji on upper gastrointestinal remodeling in streptozotocin-induced diabetic rats. World J Gastroenterol 2012; 18: 4875-4884.
[8] Nagai R, Murray DB, Metz TO, Baynes JW. Chelation: a fundamental mechanism of action of AGE inhibitors, AGE breakers, and other inhibitors of diabetes complications. Diabetes 2012; 61: 549-559.
[9] Duran-Jimenez B, Dobler D, Moffatt S, Rabbani N, Streuli CH, Thornalley PJ, Tomlinson DR, Gardiner NJ. Advanced glycation end products in extracellular matrix proteins contribute to the failure of sensory nerve regeneration in diabetes. Diabetes 2009; 58: 2893-2903.
[10] Farrugia G. Histologic changes in diabetic gastroparesis. Gastroenterol Clin North Am 2015; 44: 31-38.
[11] Yarandi SS, Srinivasan S. Diabetic gastrointestinal motility disorders and the role of enteric nervous system: current status and future directions. Neurogastroenterol Motil 2014; 26: 611-624.
[12] Vallejo D, Codocedo JF, Inestrosa NC. Posttranslational modifications regulate the postsynaptic localization of PSD-95. Mol Neurobiol 2016; [Epub ahead of print].
[13] Han K, Kim E. Synaptic adhesion molecules and PSD-95. Prog Neurobiol 2008; 84: 263-283.
[14] Tian A, Qian W, Liu S. Changes in expressions of PSD95 and Synapsin-I in rats with diabetic gastroparesis. World Chinese Journal of Digestology 2010; 14: 1417-1421.
[15] Guerci B, Bourgeois C, Bresler L, Scherrer ML, Böhme P. Gastric electrical stimulation for the treatment of diabetic gastroparesis. Diabetes Metab 2012; 38: 393-402.
[16] Ro S, Park C, Jin J, Zheng H, Blair PJ, Redelman D, Ward SM, Yan W, Sanders KM. A model to study the phenotypic changes of interstitial cells of Cajal in gastrointestinal diseases. Gastroenterology 2010; 138: 1068-1078.
[17] Gaddipati KV, Simonian HP, Kresge KM, Boden GH, Parkman HP. Abnormal ghrelin and pancreatic polypeptide responses in gastroparesis. Dig Dis Sci 2006; 51: 1339-1346.
[18] Fournel A, Marlin A, Abot A, Pasquio C, Cirillo C, Cani PD, Knauf C. Glucosensing in the gastrointestinal tract: impact on glucose metabolism. Am J Physiol Gastrointest Liver Physiol 2016; 310: G645-658.
[19] Sanger GJ, Lee K. Hormones of the gut-brain axis as targets for the treatment of upper gastrointestinal disorders. Nat Rev Drug Discov 2008; 7: 241-254.
[20] Lin XH, Wei DD, Wang HC, Wang B, Bai CY, Wang YQ, Li GE, Li HP, Ren XQ. Role of orphan G protein-coupled receptor 55 in diabetic gastroparesis in mice. Sheng Li Xue Bao 2014; 66: 332-340.
[21] Zhao J, Frøkjaer JB, Drewes AM, Ejskjaer N. Upper gastrointestinal sensory-motor dysfunction in diabetes mellitus. World J Gastroenterol 2006; 18: 2846-2857.
[22] Zhao JB, Yang J, Gregersen H. Biomechanical and morphometric intestinal remodeling during experimental diabetes in rats. Diabetologia 2003; 46: 1688-1697.
[23] Horowitz M, Samsom M. Gastrointestinal function in diabetes mellitus. John Wiley & Sons, Ltd, Chichester, England 2004.
[24] Sánchez SS, Genta SB, Aybar MJ, Honoré SM, Villecco EI, Sánchez Riera AN. Changes in the expression of small intestine extracellular matrix proteins in streptozotocin-induced diabetic rats. Cell Biol Int 2000; 24: 881-888.
[25] Chen PM, Zhao JB, Gregersen H. Up-regulated expression of advanced glycation end-products and their receptor in the small intestine and colon of diabetic rats. Dig Dis Sci 2012; 57: 48-57.
[26] Zhao J, Chen P, Gregersen H. Morpho-mechanical intestinal remodeling in type 2 diabetic GK rats--is it related to advanced glycation end product formation? J Biomech 2013; 46: 1128-1134.
[27] Guyton AC, Hall JE. Textbook of medical physiology. Tenth edition. USA: W.B. Saunders Company; 2000.
[28] Bhor VM, Sivakami S. Regional variations in intestinal brush border membrane fluidity and function during diabetes and the role of oxidative stress and non-enzymatic glycation. Mol Cell Biochem 2003; 252: 125-132.
[29] Bierhaus A, Humpert PM, Morcos M, Wendt T, Chavakis T, Arnold B, Stern DM, Nawroth PP. Understanding RAGE, the receptor for advanced glycation end products. J Mol Med (Berl) 2005; 83: 876-886.

[30] Cline H. Synaptogenesis: a balancing act between excitation and inhibition. Curr Biol 2005; 15: R203-205.
[31] Okabe S. Molecular anatomy of the postsynaptic density. Mol Cell Neurosci 2007; 34: 503-518.
[32] Kim E, Ko J. Molecular organization and assembly of the postsynaptic density of excitatory brain synapses. Results Probl Cell Differ 2006; 43: 1-23.
[33] deBartolomeis A, Fiore G. Postsynaptic density scaffolding proteins at excitatory synapse and disorders of synaptic plasticity: implications for human behavior pathologies. Int Rev Neurobiol 2004; 59: 221-254.
[34] Levinson JN, El-Husseini A. New players tip the scales in the balance between excitatory and inhibitory synapses. Mol Pain 2005; 1: 12.
[35] Petersen JD, Chen X, Vinade L, Dosemeci A, Lisman JE, Reese TS. Distribution of postsynaptic density (PSD)-95 and Ca2+/calmodulin-dependent protein kinase II at the PSD. J Neurosci 2003; 23: 11270-11278.
[36] Cook DJ, Teves L, Tymianski M. Treatment of stroke with a PSD-95 inhibitor in the gyrencephalic primate brain. Nature 2012; 483: 213-217.
[37] Yuki D, Sugiura Y, Zaima N, Akatsu H, Takei S, Yao I, Maesako M, Kinoshita A, Yamamoto T, Kon R, Sugiyama K, Setou M. DHA-PC and PSD-95 decrease after loss of synaptophysin and before neuronal loss in patients with Alzheimer's disease. Sci Rep 2014; 4: 7130.
[38] Savioz A, Leuba G, Vallet PG. A framework to understand the variations of PSD-95 expression in brain aging and in Alzheimer's disease. Ageing Res Rev 2014; 18: 86-94.
[39] Jin QH, Shen HX, Wang H, Shou QY, Liu Q. Curcumin improves expression of SCF/c-kit through attenuating oxidative stress and NF-κB activation in gastric tissues of diabetic gastroparesis rats. Diabetol Metab Syndr 2013; 5: 12.
[40] Lorincz A, Redelman D, Horváth VJ, Bardsley MR, Chen H, Ordög T. Progenitors of interstitial cells of cajal in the postnatal murine stomach. Gastroenterology 2008; 134: 1083-1093.
[41] Luo Y, Lin L, Zhang HJ, Li XL, Wu GJ, Wang MF. Changes in Cajal Interstitial cell and SCF of colon in diabetic rats. World Chinese Journal of Digestology 2007; 05: 458-463.
[42] Long QL, Fang DC, Shi HT, Xiang GC, Luo YH. Changes in SCF-Kit signal pathway and its impact on Cajal interstitial cell in DM rats. Journal of Third Military Medical University 2007; 02: 141-143.
[43] Stengel A, Rivier J, Taché Y. Modulation of the adaptive response to stress by brain activation of selective somatostatin receptor subtypes. Peptides 2013; 42: 70-77.
[44] Herszényi L, Mihály E, Tulassay Z. Somatostatin and the digestive system. Clinical experiences. Orv Hetil 2013; 154: 1535-1540.
[45] Onoue S, Misaka S, Yamada S. Structure-activity relationship of vasoactive intestinal peptide (VIP): potent agonists and potential clinical applications. Naunyn Schmiedebergs Arch Pharmacol 2008; 377: 579-590.
[46] Jiang Y, Bai X, Zhu X, Li J. The effects of Fructus Aurantii extract on the 5-hydroxytryptamine and vasoactive intestinal peptide contents of the rat gastrointestinal tract. Pharm Biol 2014; 52: 581-585.
[47] Grover M, Farrugia G, Lurken MS, Bernard CE, Faussone-Pellegrini MS, Smyrk TC, Parkman HP, Abell TL, Snape WJ, Hasler WL, Ünalp-Arida A, Nguyen L, Koch KL, Calles J, Lee L, Tonascia J, Hamilton FA, Pasricha PJ; NIDDK Gastroparesis Clinical Research Consortium. Cellular changes in diabetic and idiopathic gastroparesis. Gastroenterology 2011; 140: 1575-1585.
[48] Adeghate E, Ponery AS, Sharma AK, El-Sharkawy T, Donáth T. Diabetes mellitus is associ-ated with a decrease in vasoactive intestinal polypeptide content of gastrointestinal tract of rat. Arch Physiol Biochem 2001; 109: 246-251.
[49] Lin L, Ji M, Zhao ZQ, Zhang HJ, Lin Z. The function of different hormones in DGP rats. Modern Digestion & Intervention 2003; 8: 74-77.